Bragg Scattering of Free Electrons Using the Kapitza-Dirac Effect

Daniel L. Freimund and Herman Batelaan

Department of Physics and Astronomy, University of Nebraska–Lincoln, Lincoln, Nebraska 68588-0111

(Received 20 August 2002; published 30 December 2002)

Bragg scattering has been observed for free electrons using a standing wave of light. Both the rocking curve and the angular electron distribution have been measured. The results of a numerical simulation to the Schrödinger equation are consistent with our experimental data. Unlike the diffraction regime which uses thin crystals, the Bragg regime requires the use of thick crystals. We point out several applications in atom optics that could be realized in electron optics.

DOI: 10.1103/PhysRevLett.89.283602 PACS numbers: 42.50.Vk, 03.75.–b, 61.14.–x

In 1933, Kapitza and Dirac [1] suggested that electrons could be diffracted by a standing wave of light, a phenomenon now known as the Kapitza-Dirac effect (KDE). The light acts as a diffraction grating for the electrons, reversing the traditional roles of light and matter in a beautiful display of wave-particle duality. Early attempts to do this with electrons [2–5] were inconclusive. Explanations were offered [6–8], including Fedorov's suggestion [9,10] that only a small portion of the electron beam, the part incident at the Bragg angle, could have interacted with the laser.

The idea of KDE was then applied to atomic diffraction by a standing light wave [11], followed by atomic Bragg scattering [12]. These examples of *atomic* KDE stimulated much work in the field of atom optics. Resonant enhancement of KDE for atomic electrons as compared to free electrons made the demands on laser intensity much less stringent.

Bucksbaum *et al.* [13] showed that electrons could be deflected by light. Multiphoton ionization of atoms in a focused laser yielded electrons that were deflected into two incoherent peaks. Later, we demonstrated KDE [14] by diffracting a free beam of electrons into separate, coherent beams using a standing wave of light. In this Letter, we report Bragg scattering of electrons with KDE, which experimentally confirms the prediction of the original 1933 paper. The inherent difficulties of working in the Bragg regime are revealed, which most likely caused the inconclusive results of the earliest experiments. In this sense, we complete the story of the Kapitza-Dirac experiment, while at the same time we open the door to the study of other phenomena with free electrons that require thick crystals. Examples of these in the field of atom optics are Bloch oscillations [15], quantum chaos studies [16,17], and other time-dependent effects such as acousto-optical modulators (AOM) [18]. An application using thick crystals has been suggested [18] to make interferometers more sensitive. Improved sensitivity for interferometric gravitational sensing makes detection of the free fall of electrons and positrons a possibility [19].

The differences in physics between the diffraction and Bragg regimes can be explained using the Heisenberg uncertainty principle [9], $\Delta x \cdot \Delta p \geq \hbar/2$, and applying it to stimulated Compton scattering. This quantum effect occurs when an electron absorbs a photon and undergoes stimulated emission by another photon. It can occur only at the Bragg angle, where energy and momentum are conserved. This angle satisfies the Bragg condition, $n\lambda_{\mathrm{dB}} = d_{\mathrm{light}} \sin\theta$, where n is the diffraction order, λ_{dB} is the de Broglie wavelength of the electrons, and $d_{\mathrm{light}} = \lambda_{\mathrm{light}}/2$ is the periodicity of the standing wave of light. At the laser focus, the uncertainty of the photon momentum can be expressed, to a good approximation, as the uncertainty in the angle of propagation of the light, $\Delta\phi$ (Fig. 1). As Δx becomes smaller, the uncertainty in the angle is increased at the waist of a focused laser, and the system enters the diffraction, or Raman-Nath, regime. In this regime, an electron beam can cross a standing wave at angles far from the Bragg angle with respect to the perpendicular and still be diffracted efficiently. The resulting

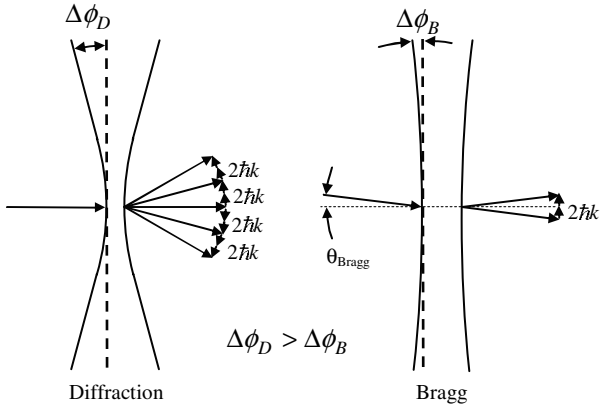

FIG. 1. Comparing two regimes of the Kapitza-Dirac effect. Electrons passing through a narrow laser waist (left) are exposed to photons with larger angular uncertainty, allowing for diffraction into many different orders. For a wide laser waist (right), momentum and energy can be conserved only for Bragg scattering.

fan of coherent diffraction orders is spaced by an angle corresponding to a transverse momentum transfer of $2\hbar k$ (Fig. 1 left). As Δx becomes larger, the system enters the Bragg regime. The increased width of the laser beam coincides with a decrease in divergence. With photons available at fewer angles, fewer diffraction orders can be reached, and the incident electron beam must cross the standing wave close to the Bragg angle (Fig. 1 right).

The motion of electrons in a standing wave of light [20] is governed by the Hamiltonian,

$$H = -\frac{\hbar^2}{2m}\frac{\partial^2}{\partial x^2} + V_o \cos^2(kx), \tag{1}$$

where V_o is the ponderomotive potential, which is related to the laser intensity of one counterpropagating beam for linearly polarized light by

$$V_o = \frac{2e^2 I}{\varepsilon_o c \omega^2 m}. \tag{2}$$

The solution of the Schrödinger equation can take the form

$$\varphi = \sum_n c_n e^{2i(n+n_o)kx}, \qquad n = 0, \pm 1, \pm 2, \ldots, \tag{3}$$

which describes the electron's behavior in the transverse direction in terms of plane waves separated by two photon recoils, $2\hbar k$, with an initial transverse momentum of $2n_o$ photon recoils. The Schrödinger equation can be manipulated through trigonometric identities and the removal of constant potential terms to find the amplitudes, c_n, through a system of differential equations

$$i\frac{dc_n}{dt} = \frac{2\hbar k^2}{m}(n^2 + 2nn_o)c_n + \frac{V_o}{4\hbar}(c_{n-1} + c_{n+1}). \tag{4}$$

In the limit as $(n\hbar k)^2/m \ll V_o$, the system is in the diffraction regime, and the solution for the amplitudes c_n is proportional to Bessel functions, leading to

$$|c_n|^2 = J_n^2\left(\frac{\mathrm{V}_o t}{\hbar}\right). \tag{5}$$

This shows that electrons incident at any arbitrary angle will scatter into the nth order with a probability equal to J_n^2. Conversely, when $(n\hbar k)^2/m \gg V_o$, the system is in the Bragg regime, and the amplitudes are proportional to sine and cosine functions, leading to

$$|c_{+1}|^2 = \cos^2\left(\frac{V_o t}{4\hbar}\right); \qquad |c_{-1}|^2 = \sin^2\left(\frac{V_o t}{4\hbar}\right). \tag{6}$$

The electrons that are incident exactly at the $+1$st order are scattered only into the -1st order, where the $+1$st order is at the Bragg angle, $\hbar k/p$, p being the total electron momentum. Similar relations hold for higher integer orders. Note that the product of the potential V_o and the interaction time t, $V_o t/\hbar$, plays the role of the interaction strength in both the diffraction and Bragg regimes. The value of this product equals about unity in our experiments to ensure an appreciable scattering probability [20]. In between these regimes, an analytical solution can be found [21]. To be capable to average over experimental parameters, we use a numerical solution.

The main difference in the experimental setups used for observation of diffraction [11] and Bragg scattering involves the beam width of the Nd:YAG laser at the region where it interacts with the electrons. This seemingly straightforward change of a parameter caused a significant experimental obstacle. The Bragg angle needs to be found, a task usually achieved by rotating the mirror that reflects the laser to create the standing wave. Because of the high intensity of the laser and its short coherence length, the use of a mirror would be problematic. Therefore, the standing wave is formed by counterpropagating two laser beams formed by a beam splitter. We found that rotating the standing wave by optical means was difficult because the overlap of the laser beams and the quality of the standing wave was hard to maintain. Instead, we rotated the vacuum system containing the electron gun relative to the optics. In the diffraction experiment, the laser is focused with a spherical lens to a 125 μm diameter. For the Bragg case, the laser beam is focused with a cylindrical lens to a width of 8 mm and a height of about 200 μm. This effectively increases the cross-sectional area of the laser focus, lowers the intensity of the beam by 2 orders of magnitude, and increases the interaction time by 2 orders of magnitude.

The pressure of our vacuum system is about 10^{-8} torr. The inside of the vacuum chamber has a double-walled, highly permeable metal tube to shield the earth's magnetic field down to less than 5 mG. The electron source is set to emit 380 eV electrons that are collimated by three molybdenum slits: two vertical slits with widths of 10 and 25 μm separated by 25 cm, followed 5 cm downstream by a 100 μm wide horizontal slit. The standing wave formed by the laser passes 1 cm behind the horizontal slit. Profiles of the electron beam are scanned with a fourth slit that is 10 μm wide, which is located 24 cm after the laser beam.

We use an Nd:YAG laser which produces 6 ns long pulses at 50 Hz. A first harmonic generation crystal is used to up-convert to light of 532 nm wavelength. The maximum average power output is 14 W. The power of the laser is adjusted by the combination of a polarizing beam splitting cube and a $\frac{1}{2}$ wave plate; it is attenuated down to 1.4 W. Two mirrors guide the laser to a beam splitter, and then each beam is guided by a mirror through a cylindrical lens. This lens focuses the laser beam in the vertical direction but does not affect the angle between the light and electrons. The transmission efficiency of the optics up to this point is 87%. The converging beams each pass through crown glass windows to enter the vacuum system where their height is focused to 200 μm to achieve an intensity of 0.3 GW/cm^2.

A time-to-amplitude converter (TAC) sends pulses to a pulse height analyzer that records time spectra taken at

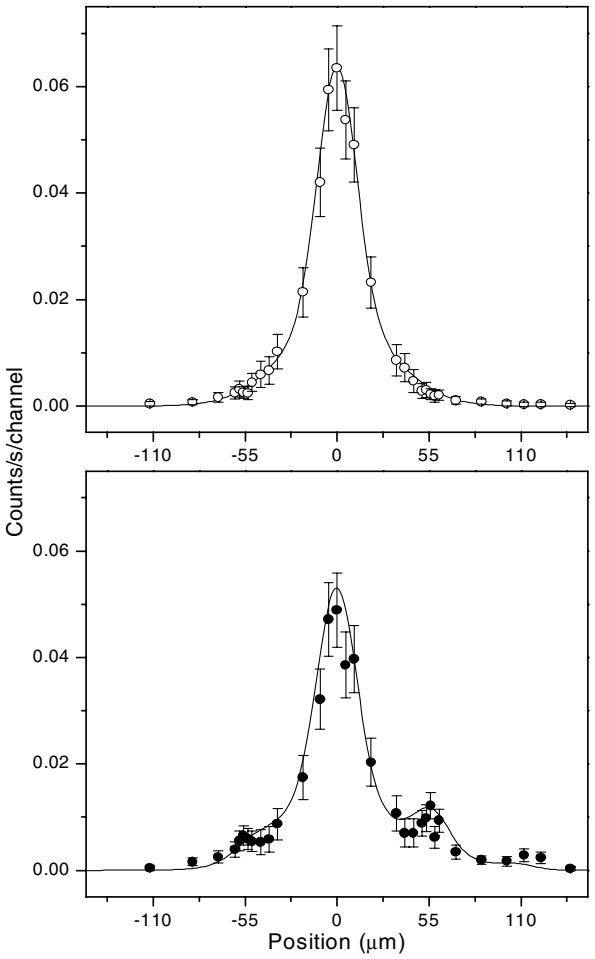

FIG. 2. Top: the electron beam profile with the laser beam off. Bottom: when the laser light is on, the electrons which are incident at the Bragg angle, with a transverse momentum component of $-1\hbar k$, are scattered to the positive first order.

varying positions along the electron beam profile. The start pulse for the TAC is detected by a photodiode that detects the laser. The stop pulse is detected by a channel electron multiplier. By taking the region of interest of the time spectra when the laser is on, the effect of the laser on the electrons can be determined.

Figure 2 shows the electron profile as a function of position. The diffraction angle, 0.2 mrad, corresponds to an electron traveling over 24 cm and being detected at a transverse displacement of 55 μm. The data show a reduced count at the zero order peak position and an increased count at the positive first order peak position. There is a small amount of electron signal found in the negative first order and the positive second orders, as well. This indicates that we have just entered the Bragg regime but are not deeply in it. Below, we explain why we believe this the best we have been capable of achieving.

Theoretical fits to these data can be found with several different combinations of laser width and incident angle. The electron distribution in Fig. 2 is insufficient to determine an unambiguous solution. To find the correct

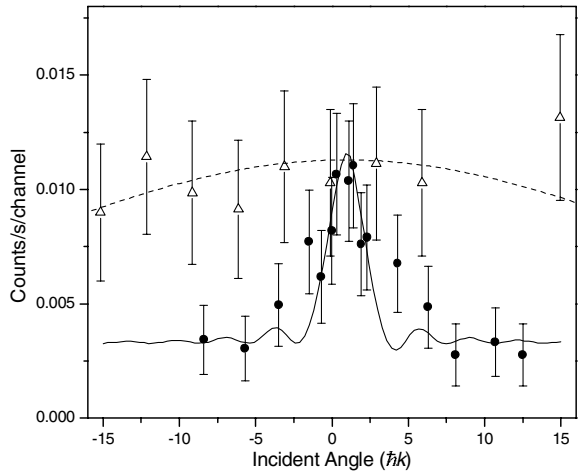

FIG. 3. The qualitative difference between the dependence on incident angle for a focused laser beam (triangles) and an unfocused laser beam (dots) shows that the Bragg regime is approached. The dotted and solid lines are theoretical calculations.

incident angle, i.e., the Bragg angle, rocking curve data are collected (Figs. 3 and 4). This was obtained by changing the relative angle between the electron beam and the laser beam while keeping the detector position fixed. To achieve this, the whole vacuum system, including the electron source, is rotated with respect to the laser and the optics.

The rocking curves of Fig. 3 show the dependence of the positive 1st order diffraction signal on incident angle. It reveals the major difference in the Bragg and diffraction regimes. In the Bragg regime, the profile appears as a narrow peak centered on the Bragg angle. This is because there are no other angles that lead to conservation of energy and momentum. In the diffraction regime, which

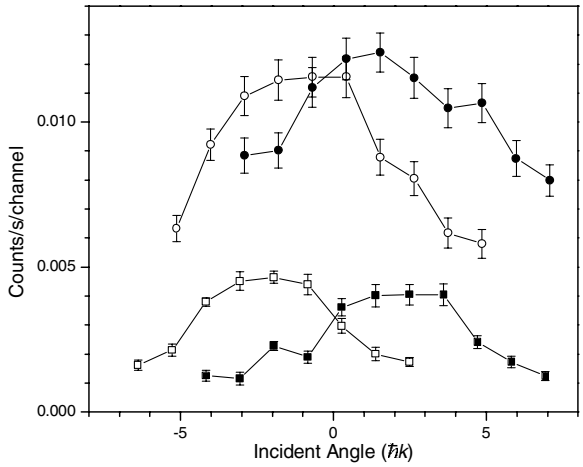

FIG. 4. Experimental data of the rocking curves for the +1st (open circles) and the −1st (closed circles) orders at 5 W and the +2nd (open squares) and the −2nd (closed squares) at 9 W. The centers of the 2nd order rocking curves are approximately twice as far apart as those of the 1st order, as they should be.

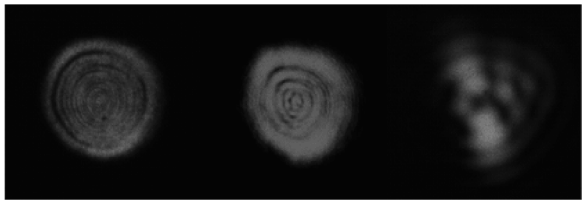

FIG. 5. The laser beam profile of the Nd:YAG at distances of 0.5, 2.8, and 17 m from the laser port is given left to right, respectively. The beam diameter for the left figure is 8 mm.

has more laser beam divergence, the profile is approximately flat over many angles of incidence. This excludes the possibility that we are observing diffraction at large angles of incidence and removes the ambiguity mentioned above. The dotted and solid lines are numerical integrations of Eq. (1). Figure 4 includes the rocking curves of the 1st and 2nd orders in the Bragg regime. The angle where the electrons enter the light at normal incidence occurs at the crossing point of the positive and negative 1st order curves and at the crossing point of the 2nd order curves. Therefore, the data allow us to calibrate the incident angle of the electrons with respect to the laser. To determine the correct angle, we use the 2nd order Bragg data because the separation of the 1st order curves is smaller and gives a less accurate result. Using this calibration of the Bragg angle, a fit to the data of Fig. 3 gives a laser width of 0.8 mm and a laser power of 0.2 W. Using these values with an incident angle of $-1\hbar k$, a theoretical curve is produced that fits the electron beam profile in the Bragg regime, as indicated in Fig. 2.

The theoretical calculation is in qualitative agreement with the experimental observation. However, note that the parameter used for the laser width is theoretically 0.8 mm while experimentally it is 8 mm. We believe that this discrepancy is partly due to the poor quality of our unfocused laser beam (Fig. 5) and partly due to alignment difficulties with unfocused laser beams. The laser beam $1/e^2$ divergence of about 0.5 mrad is identical to our factory specifications (Continuum Powerlite 9050) but corresponds to a laser focus waist of 3.1 mm, which includes our measured M^2 of 2.32. Attempts to spatially filter the laser beam failed due to high intensity. Also, note that the virtual focus would lie 16 m before the interaction region. In the theoretical calculation, we assume that interaction takes place in the laser focus. Complex descriptions of the actual laser light spatial and angular distribution appear to be necessary to obtain a better agreement between the experimental and theoretical parameters for the laser width.

Our realization of Bragg scattering shows that free electron interaction with thick light crystals is possible. This allows for the possibility to explore analogies between atom optics and electron optics; in particular, time-dependent modulations of the standing wave seem promising. An example of this is an electron AOM that, if realized, could be used as a fast electron beam switch or as an electron frequency shifter. Another analogy that may be explored follows atom interferometry. Using Bragg scattering as a beam splitter offers some advantages [22] as compared to using diffraction [23].

We thank Ben Williams and Les Marquart for designing and building the accurate rotational mount for our system, and Mark Rosenberry for useful discussions. This work is funded by NSF, the Research Corporation, NRI, and DOD EPSCoR.

[1] P. L. Kapitza and P. A. M. Dirac, Proc. Cambridge Philos. Soc. **29**, 297 (1933).
[2] H. Schwarz, Z. Phys. **204**, 276 (1967).
[3] L. S. Bartell, R. R. Roskos, and H. B. Thompson, Phys. Rev. **166**, 1494 (1968).
[4] Y. Takeda and I. Matsui, J. Phys. Soc. Jpn. **25**, 1202 (1968).
[5] H. Chr. Pfeiffer, Phys. Lett. **26A**, 362 (1968).
[6] M. M. Nieto, Am. J. Phys. **37**, 162 (1969).
[7] H. De Lang, Opt. Commun. **4**, 191 (1971).
[8] H. Schwarz, Phys. Lett. **43A**, 457 (1973).
[9] M.V. Fedorov, in *Laser Science and Technology; An International Handbook,* edited by V.S. Letokhov (Harwood, New York, 1991), Vol. 13, Chap. 4, p. 22.
[10] M.V. Fedorov, Opt. Commun. **12**, 205 (1974).
[11] P. L. Gould, G. A. Ruff, and D. E. Pritchard, Phys. Rev. Lett. **56**, 827 (1986).
[12] P. J. Martin, B. G. Oldaker, and D. E. Pritchard, Phys. Rev. Lett. **60**, 515 (1988).
[13] P. H. Bucksbaum, D.W. Schumacher, and M. Bashkansky, Phys. Rev. Lett. **61**, 1182 (1988).
[14] D. L. Freimund, K. Aflatooni, and H. Batelaan, Nature (London) **413**, 142 (2001).
[15] M. B. Dahan, E. Peik, J. Reichel, Y. Castin, and C. Salomon, Phys. Rev. Lett. **76**, 4508 (1996).
[16] J. C. Robinson, C. F. Bharucha, K.W. Madison, F. L. Moore, B. Sundaram, S. R. Wilkinson, and M. G. Raizen, Phys. Rev. Lett. **76**, 3304 (1996).
[17] D. A. Steck, V. Milner, W. H. Oskay, and M. G. Raizen, Phys. Rev. E **62**, 3461 (2000).
[18] S. Bernet, R. Abfalterer, C. Keller, M. K. Oberthaler, J. Schmiedmayer, and A. Zeilinger, Phys. Rev. A **62**, 023606 (2000).
[19] M. M. Nieto and T. Goldman, Phys. Rep. **205**, 221 (1991).
[20] H. Batelaan, Contemp. Phys. **41**, 369 (2000).
[21] M.V. Fedorov, JETP **52**, 1434 (1967).
[22] D. M. Giltner, R.W. McGowan, and S. A. Lee, Phys. Rev. Lett. **75**, 2638 (1995).
[23] E. Rasel, M. K. Oberthaler, H. Batelaan, J. Schmeidmayer, and A. Zeilinger, Phys. Rev. Lett. **75**, 2633 (1995).